Controlling vortex motion and chaotic advection

Bernd R. Noack[1] Igor Mezić[2] and Andrzej Banaszuk[1]
[1]United Technologies Research Center,
East Hartford, CT 06108, USA
[2]Division of Engineering and Applied Sciences,
Harvard University, Cambridge, MA 02138, USA

Abstract

Effects of time-dependent forcing on the flow induced by a single vortex in a corner are studied. The objective of forcing is to maximize flux across the separating streamline in the flow while keeping the position of the vortex bounded within a prescribed domain. Concepts of chaotic advection and control theory are used to achieve this goal. Transformation into flat coordinates is employed to prove controllability using various actuation methods. Flat coordinates also alleviate the search for the optimal (flux-maximizing) vortex trajectory. A feedback law is designed to stabilize this trajectory. Mixing in the optimized flow is studied.

1 Introduction

In the last two decades, much progress has been made in employing dynamical systems theory to laminar mixing [1, 16, 21]. In much of this work the emphasis has been on *understanding the mechanisms* of mixing in laminar flows. For example Melnikov theory and associated lobe dynamics have been used to study transport and mixing in and out of the recirculation bubble of the vortex Batchelor couple in a pioneering study of Rom Kedar et al [18]. Those mechanisms are now well-understood in two-dimensional flows and partially in three-dimensional flows [12, 9]. In this study we pursue a related question of *optimizing and controlling* transport and mixing in two-dimensional flows. Akin to first chaotic advection studies we chose a simple vortex model - a single vortex in a corner subject to a potential field. The motivation for this study comes from flows in a combustor recirculation zone. In the absence of time-dependent forcing (introduced by modulating the potential field) the vortex is either at a stable equilibrium position or is moving on a periodic trajectory in the plane.

The first question that we ask is: if we allow for the arbitrary time-modulation of the potential field, can we move the vortex from an arbitrary initial position to an arbitrary final position in the plane? The answer to this question is shown to be positive using the transformation to the so-called *flat coordinates* [15, 8]. Having this result, we can proceed to search over all the trajectories of the vortex in a bounded domain of the plane and determine the optimal one with respect to a suitable measure. In this paper we choose this measure to be the flux through the separatrix, thus linking control theory and chaotic advection theory. Once the optimal trajectory is found, we stabilize it using a feedback law. The search for the optimal trajectory is pursued here using the numerical simplex method. Various characterizations of mixing utilizing dynamical systems concepts can now be pursued.

2 The point vortex model

In this section, the vortex model for the recirculation region is outlined generalizing an analytical study of unforced flow by Suh [19].

The flow is described in a Cartesian coordinate system x,y of which the origin coincides with the corner. The walls of the corner lie on the x- and y-axes and the considered domain is the first quadrant $D = \{(x, y) : x \geq 0,\ y \geq 0\}$. The independent variables are the location $x = (x, y)$ and the time t. The x- and y- components of the velocity field $\mathbf{u}$ are denoted by u and v, respectively. The potential corner flow is expressed by the stream function

$$\Psi_p(\mathbf{x}) = k\, x\, y, \tag{1}$$

or, equivalently, the velocity field $u = \partial_y \Psi_p = k\, x$, $v = -\partial_x \Psi_p = -k\, y$. The constant k specifies the magnitude of the velocity at a given location.

A vortex with circulation $-\Gamma$, where $\Gamma > 0$, is placed at $\mathbf{x}_v = (x_v,\ y_v)$. The negative sign of the circulation indicates that the induced fluid motion rotates in clockwise direction. The no penetration condition at the walls is enforced by mirror vortices in quadrants 2, 3 and 4 at $\mathbf{x}_2 = (-x_v,\ y_v)$, at $\mathbf{x}_3 = (-x_v, -y_v)$, and at $\mathbf{x}_4 = (x_v,\ -y_v)$, respectively. The circulation of the mirror vortex in quadrant n is given by $\Gamma_n = (-1)^n\, \Gamma$. For reasons of simplicity, the position and circulation of vortex in the domain is also denoted by $\mathbf{x}_1 = \mathbf{x}_v$ and

$\Gamma_1 = -\Gamma$ in the sequel.

The motion of the real vortex is determined by the potential corner flow and the velocity field induced by the mirror vortices. The stream function of the induced field at location $\mathbf{x}$ is

$$\Psi_{\rm mv}(\mathbf{x}, \mathbf{x}_v) = \sum_{n=2}^{4} \frac{\Gamma_n}{2\pi} \ln \|\mathbf{x} - \mathbf{x}_n\|, \qquad (2)$$

where $\|\mathbf{x} - \mathbf{x}_n\|$ represents the Euclidean distance between the location and the mirror vortex n. The stream function can be considered a function of the the location $\mathbf{x}$ and the vortex position $\mathbf{x}_v$, since the positions of all mirror vortices are slaved to the real vortex at each instant.

Actuation is provided by the free-stream perturbation $\epsilon\Psi_c$, where ϵ represents the forcing amplitude and Ψ_c the free stream,

$$\Psi_c(\mathbf{x}) = k\, x\, y. \qquad (3)$$

The evolution equation for the vortex position reads

$$\dot{\mathbf{x}}_v = \mathbf{f}(\mathbf{x}_v) + \epsilon\, \mathbf{g}(\mathbf{x}_v). \qquad (4)$$

and contains the velocity field due to the natural dynamics $f = (\partial_y [\Psi_p + \Psi_{\rm mv}], -\partial_x [\Psi_p + \Psi_{\rm mv}])|_{\mathbf{x}=\mathbf{x}_v}$ and the actuation field $g = (\partial_y \Psi_c, -\partial_x \Psi_c)|_{\mathbf{x}=\mathbf{x}_v}$. At $\epsilon \equiv 0$, the evolution equation has the form of an autonomous system. Otherwise, time-dependence due to ϵ enters in a simple form which is well investigated in control theory. Employing Eqs. (1),(2),(4) yields

$$\dot{x}_v = +k\,(1+\epsilon)\, x_v + \gamma \left(-\frac{1}{y_v} + \frac{y_v}{r_v^2}\right), \qquad (5)$$

$$\dot{y}_v = -k\,(1+\epsilon)\, y_v + \gamma \left(+\frac{1}{x_v} - \frac{x_v}{r_v^2}\right), \qquad (6)$$

where $r_v = \sqrt{x_v^2 + y_v^2}$ and $\gamma = \Gamma/4\pi$. The equations can be simplified by non-dimensionalization with length scale $L = \sqrt{\Gamma/8\pi k}$ and time scale $T = 1/2k$, yielding

$$\dot{x}_v = \frac{1}{2}\,(1+\epsilon)\, x_v - \frac{1}{y_v} + \frac{y_v}{r_v^2},$$
$$\dot{y}_v = -\frac{1}{2}\,(1+\epsilon)\, y_v + \frac{1}{x_v} - \frac{x_v}{r_v^2}. \qquad (7)$$

Note that for $\epsilon = 0$ the streamfunction (or Hamiltonian) for the velocity field (7) is given by

$$\Psi = \frac{x_v y_v}{2} + \ln(\frac{x_v}{y_v}) + \ln\sqrt{(x_v^2 + y_v^2)}. \qquad (8)$$

In the sequel, we assume all quantities to be non-dimensionalized correspondingly and use the original symbols for reasons of simplicity

In addition to free-stream forcing, several local actuations with associated stream function $\epsilon\,\Psi_c$ were studied. The actuators are sources (sinks) when the amplitude ϵ is positive (negative). The no-penetration condition is violated at the actuator position and is enforced elsewhere by mirror sources. The studied actuator configurations include (a) a source at the origin,

$$\Psi_c(\mathbf{x}) = \arctan\left[\frac{y}{x}\right], \qquad (9)$$

(b) a source at positive x-axis $(c, 0)$ with the corresponding image at $(-c, 0)$,

$$\Psi_c(\mathbf{x}) = \arctan\left[\frac{y}{x-c}\right] + \arctan\left[\frac{y}{x+c}\right], \qquad (10)$$

and (c) zero-net flux source-sink combination at $(0, c)$ and $(c, 0)$ with corresponding images,

$$\Psi_c(\mathbf{x}) = \arctan\left[\frac{y-c}{x}\right] + \arctan\left[\frac{y+c}{x}\right] + \arctan\left[\frac{x}{y-c}\right] + \arctan\left[\frac{x}{y+c}\right]. \qquad (11)$$

The dynamics of the fluid is parametrized by the motion of the vortex. The motion of a fluid particle with position $x_{\rm fp}$ is given by

$$\dot{\mathbf{x}}_{\rm fp} = (\partial_y \Psi, -\partial_x \Psi)\Big|_{\mathbf{x}=\mathbf{x}_{\rm fp}} \qquad (12)$$

where $\Psi = \Psi_p + \Psi_v + \epsilon\,\Psi_c$. The velocity field induced by the four vortices and the time-dependent strain field has the streamfunction expressed by

$$\Psi(\mathbf{x}_{\rm fp}, \mathbf{x}_n, \epsilon) = \Psi_v(\mathbf{x}_{\rm fp}, \mathbf{x}_n) + (1+\epsilon)\,\Psi_c(\mathbf{x}_{\rm fp})$$
$$= \sum_{n=1}^{4} \frac{\Gamma_n}{2\pi} \ln\|\mathbf{x}_{\rm fp} - \mathbf{x}_n\| + (1+\epsilon) k x_{\rm fp} y_{\rm fp}. \qquad (13)$$

Similar expressions are valid for the alternative actuation fields stated above.

Note that this problem which is based on point vortex model of the velocity field carries many of the properties of the "real" fluid mixing problem where by "real" we mean the problem posed within the context of Navier-Stokes equations. The control ϵ enters in the vortex motion equation (7) the way it would enter into Navier-Stokes. On the other hand, we are interested in changing the properties of (13), not (7). The control affects (13) both directly through the input ϵ and indirectly, by changing the original velocity field as the position of the vortex has changed.

3 Vortex motion

The vortex position $(x_{v0}, y_{v0}) = (1, 1)$ is readily seen to be a fixed point of Eqs. (7). At this point, the induced

velocity of the mirror vortices is equal but opposite to the potential corner flow. In non-normalized coordinates, this fixed point is expressed by $x_{v0} = y_{v0} = \sqrt{\gamma/2k}$, i.e. the distance between the fixed point and the origin increases with the strength of the vortex and decreases with the magnitude of the potential corner flow, as intuitively clear. It is a simple exercise to show that there exist no further fixed points in the domain $x_v, y_v > 0$.

The dynamics of the infinitesimal perturbation x' around x_{v0} is described by

$$\dot{x}'_v = -y'_v, \qquad \dot{y}'_v = x'_v.$$

The fixed point is hence a marginally stable center and small perturbations have angular frequency $\omega = 1$. The dimensional value of the frequency $\omega = 2k$ increases with potential flow magnitude and is independent of the circulation.

The linearization of the vector field calculated in the previous section shows that the critical point $(x_{v0}, y_{v0}) = (1, 1)$ of the streamfunction is not singular. In fact, trajectories close to the fixed point must be periodic orbits. By the fact that the topological type of the intersections of constant planes with the streamfunction changes only at critical points, all of the trajectories in the first quadrant of the plane (excluding the axis) have to be periodic orbits. The velocity $\dot{x}_v$ can be zero only if $y_v \leq 1$ and by symmetry around $x_v = y_v$, $\dot{y}_v$ can be zero only if $x_v \leq 1$. These properties are reflected in numerical solutions of Eqs. (7) that are shown in figure 1 - the computed orbits are periodic trajectories around the fixed point with clockwise orientation.

From simulations we observe that the period $T_{\rm per}$ of the vortex motion increases with the amplitude of oscillation which is defined as the maximum distance of the orbit from the fixed point,

$$R: = \max_{\forall t} \|\mathbf{x}_v(t) - \mathbf{x}_{v0}\|. \tag{14}$$

At $R \leq 0.5$, this relationship is approximately described by $T_{\rm per} = 2\pi\,(1 + 0.24R^2)$. This increase is a useful fact in considerations of forced vortex motion. In particular, consider time-periodic forcing given by $\epsilon(t) = \epsilon(t + \tau), |\epsilon| < \delta$. Then, using Moser's version of the KAM theorem [2] it can be shown, using the fact that $\partial T_{\rm per}/\partial R > 0$ that most of the quasi-periodic orbits of the related Poincaré map persist in the forced case for small enough δ. In other words, for small enough control the vortex motion will be quasi-periodic starting from most initial conditions. A simple consequence of this is that, for small control, vortex that starts at the equilibrium point will not drift far from it at any time. However, the motion of the vortex can become chaotic starting from some initial conditions

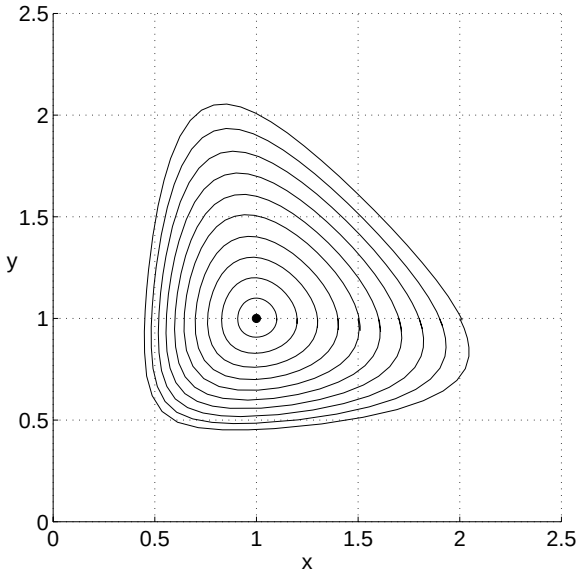

Figure 1: *Orbits associated with natural periodic vortex motion. The bullet at* $(1,1)$ *indicates the fixed point.*

- those that are close to resonant periodic orbits for which the period of unforced motion and the period of the forcing are rationally related.

In the pioneering mixing study of Rom-Kedar, Leonard and Wiggins [18], actuation of the vortex pair is assumed to be periodic with periodic forcing $\epsilon = A \sin \Omega t$. In the present study, we want to prescribe a much larger class of vortex motion by control laws for actuation as a function of time and vortex position, $\epsilon = \epsilon(x_v, y_v, t)$. This class includes periodic motion at arbitrary frequencies and at arbitrary not necessarily small amplitudes. The goal can be achieved in the framework of control theory. The key element of the strategy is finding a transformation into the so-called flat coordinates [15, 8]

$$z_1 = \alpha_1(x_v, y_v), \qquad z_2 = \alpha_2(x_v, y_v) \tag{15}$$

such that Eqn. (4) can be expressed in the form

$$\dot{z}_1 = z_2, \qquad \dot{z}_2 = p(z_1, z_2) + \epsilon\, q(z_1, z_2). \tag{16}$$

Thus, the first flat coordinate can be prescribed by an arbitrary function of time $z_1 = z_1^d(t)$. The first derivative corresponds to the second flat coordinate $z_2^d = \dot{z}_1^d$. Eqn. (16) represents the controlled vortex dynamics and any such vortex motion $(z_1^d,\ z_2^d)$ is easily seen to arise by imposing the control law

$$\epsilon = \frac{\dot{z}_2^d - p(z_1^d, z_2^d)}{q(z_1^d, z_2^d)} \tag{17}$$

provided that $q \neq 0$.

Differentiation of the first coordinate (15) employing

Eqn. (4) yields

$$\dot{z} = L_f \alpha_1 + \epsilon\, L_g \alpha_1 \tag{18}$$

with Lie derivatives $L_f \alpha_1 = f_1\, \partial_{x_v} \alpha_1 + f_2\, \partial_{y_v} \alpha_1$ and $L_g \alpha_1 = g_1\, \partial_{x_v} \alpha_1 + g_2\, \partial_{y_v} \alpha_1$. Comparing Eqn. (18) and (16) implies $L_g \alpha_1 \equiv 0$ and $z_2 = L_f(x_v, y_v)$, since the first transformed equation (16) does not contain ϵ. Geometrically, the first condition requires that the gradient of the flat coordinate z_1 is everywhere perpendicular to the forcing field g, or, equivalently, that z_1 is a function of the (non-dimensionalized) stream function $\Psi_c = \frac{1}{2} x_v\, y_v$.

Equations (7) can be brought into flat form by straightforward computations. The transformation is given by

$$z_1 = x_v\, y_v, \qquad z_2 = \frac{y_v^2 - x_v^2}{r_v^2}, \tag{19}$$

the inverse map being

$$x_v = z_1 \left(\frac{1 - z_2}{1 + z_2}\right)^{1/4}, \quad y_v = z_1 \left(\frac{1 + z_2}{1 - z_2}\right)^{1/4}. \tag{20}$$

The dynamics in flat coordinates is described by

$$\dot{z}_1 = z_2, \quad \dot{z}_2 = p + \epsilon q, \tag{21}$$

where $p = -4\, x_v\, y_v\, (x_v\, y_v - 1)/r_v^4$ and $q = -4\, x_v^2\, y_v^2/r_v^4$. Vortex motion is controllable: if we want the vortex to go from an arbitrary point (z_{10}, z_{20}) to (z_{1T}, z_{2T}) during the time T, we can prescribe a function $z_1^d(t)$ such that $z_1^d(0) = z_{10}, \dot{z}_1^d(0) = z_{20}$ and $z_1^d(T) = z_{1T}, \dot{z}_1^d(T) = z_{2T}$. Then controllability follows by applying the control law (17), since q does not vanish in the domain $x_v, y_v > 0$.

The control law (17) has to be enhanced by stabilizing feedback terms to account for transient behaviour,

$$\epsilon = \frac{\dot{z}_2^d - p(z_1, z_2) - k_1(z_1 - z_1^d) - k_2(z_2 - z_2^d)}{q(z_1, z_2)}. \tag{22}$$

The coefficients k_1, k_2 must be chosen such that the deviations $e_1 = z_1 - z_1^d$, $e_2 = z_2 - z_2^d$ tend to zero with increasing time. For this, it is sufficient to choose $k_1 > 0$ and $k_2 > 0$.

4 An optimal mixing problem

The instantaneous flow is determined by the vortex position. The fluid motion is typically characterized by streamlines, pathlines and streaklines. Under steady-state conditions, i.e. $x_v = x_{v0}$, $\epsilon = 0$, all three kinds of curves coincide.

Under periodic conditions, i.e. at natural or controlled periodic vortex motion, the fluid motion may be characterized by the Poincaré map $x^\star = \Phi_T(x)$, where x represents the initial position of the fluid particle and $x^\star$ the position one period T_{per} later. At small amplitudes, the Poincaré map has (at least) three fixed points, one at the origin, one x_s on the x-axes and one x_u on the y-axis (see Fig. 2) as the hyperbolic points of the Poincaré map persist under perturbation. The fixed point x_s (x_u) has a stable (unstable) manifold $W_s(x_s)$ ($W_u(x_u)$) extending into the domain. The manifolds intersect each other infinitely many times near the fixed points [10]. Fixed points and invariant manifolds can be shown to be symmetric with respect to the $x = y$ bisector, if the vortex motion has the same symmetry and if the initial position of the vortex is on the $x = y$ line. We define a curve C which consists of the sections of the invariant manifolds from the fixed points to the first intersection point (Fig. 2) [18]. For the considered parameters, the curve is nearly circular. In Sec. 5, further implications of the Poincaré map on mixing dynamics will be discussed. The recirculation region R shall be defined by the region bounded by the x- and y-axis and C. In the limit of small amplitudes R, the curve C converges to the steady state separatrix.

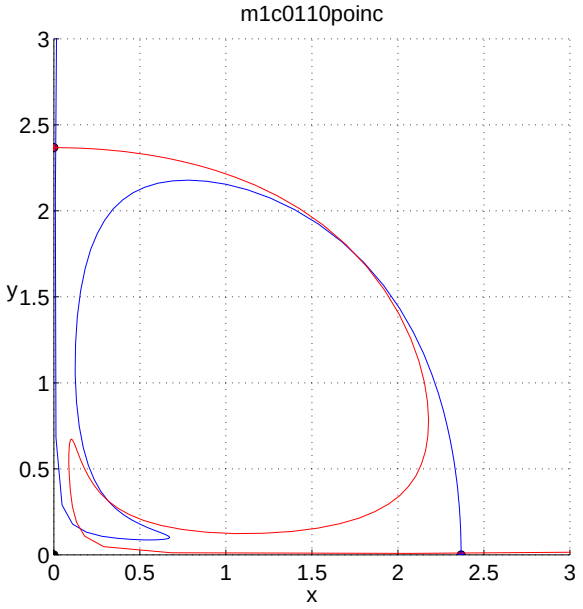

Figure 2: *Principal sketch of the Poincaré map. The associated controlled vortex motion has sinusoidal flat coordinate* $z_1 = 1 + A \sin \Omega t$ *at* $\Omega = 1$ *and* $R = 0.1$.

Mixing is associated with the behaviour of an ensemble of fluid particles over a finite period of time. In a Hamiltonian system such as (12) it is known from numerical simulation that in the region near the separatrix good mixing occurs for unsteady perturbations of steady flows [21]. In particular it can be rigorously proven that some particles exhibit chaotic behavior. Kolmogorov-Sinai entropy - which is for two-dimensional systems the integral of positive Lyapunov

exponent over area - was recently introduced as a measure of mixing in zones where flow is chaotic [7]. This quantity is, in the case of small unsteady perturbations to a steady flow, monotonically related to the flux over one period (which is the size of the lobe) and in turn to Melnikov integral [20]. Thus mixing will be increased if the size of the fluid exchange across C is increased. The instantaneous rate of fluid exchange is quantified by

$$\Phi_{inst} = \int_C ds\, |u_n|$$

where ds represents an arc element of C and u_n the normal component of the velocity. A suitable mixing measure Φ may be defined by the flux averaged over one period and normalized with the area $|R|$,

$$\Phi = \frac{1}{T_{\rm per}\,|\mathcal{R}|} \int_0^{T_{\rm per}} dt \int_C ds\, |u_n|. \qquad (23)$$

Φ vanishes under steady-state conditions. $1/\Phi$ has the dimension of a time. This time is an order-of-magnitude estimate of the period during which most of the untrapped fluid may be expected to be exchanged by new fluid.

In the optimal mixing problem, vortex motion is assumed to be periodic and bounded. The restriction to periodic motion significantly simplifies the solvability of the problem. The requirement of boundedness is motivated by engineering interest to limit the level of unsteadiness. Let $V(R_{\max}, T_{\rm per})$ be the set of all controlled vortex motions $x_v(t)$ which satisfy the following three conditions: **C1:** The vortex motion has period $T_{\rm per} = 2\pi/\Omega$, i.e. $x_v(t + T_{\rm per}) = x_v(t)$ for all t; **C2:** The vortex motion is bounded by a circle of radius $R_{\max}$ around the fixed point x_{v0}, i.e. $R \le R_{\max}$ where R is defined in Eqn. (14). **C3:** The vortex motion satisfies the evolution equations (7) with control law (22). We want to find the optimal vortex motion $x_v^{\rm opt} \in V(R_{\max}, T_{\rm per})$ which maximizes the flux (23), i.e.,

$$\Phi(\mathbf{x}_v^{\rm opt}) = \sup_{\mathbf{x}_v \in \mathcal{V}(R_{\max}, T_{\rm per})} \Phi(\mathbf{x}_v).$$

This optimization problem may be re-formulated exploiting the controllability, i.e. that the vortex motion is parametrized by the flat coordinate z_1: Let $Z(R_{\max}, T_{\rm per})$ be the set of all differentiable functions with period $T_{\rm per} = 2\pi/\Omega$ and for which the associated vortex motion[1] satisfies C2. Find the optimal flat output trajectory $z_1^{\rm opt} \in Z(R_{\max}, T_{\rm per})$, which maximizes the flux of the associated vortex motion.

The optimal mixing problem is likely to have no global solution for the following physical reason. Assume $x_v^{\rm opt} \in V(R_{\max}, T_{\rm per})$ has the largest flux. Then, a vortex motion with a large multiple of the frequency of $x_v^{\rm opt}$ can be expected to induce a still larger flux, since more actuation is required at higher frequency and the actuation also contributes to the flux. Similarly, low-amplitude high-frequency wiggles may lead to large actuations ϵ and hence contribute to the flux. However, there is numerical evidence for the existence of local maxima in a suitable finite-dimensional subspace, i.e. there exist vortex trajectories such that every small perturbation of this trajectory leads to a smaller flux. In the sequel, only these local maxima are considered. This problem is avoided if a bound on actuation size (i.e. the magnitude of $|\epsilon|$ is also specified.

[1] The vortex position $\mathbf{x}_v(t)$ is obtained from $(z_1, z_2) = (z_1, \dot{z}_1)$ via the inverse transformation (20).

Table 1: *Results of the optimal mixing problem: The first two rows contain the parameters for the side constraints. $\Phi^{(N)}$ represents the flux of the locally optimal vortex motion based on a truncated Fourier expansion up to N-th harmonics (24).*

Ω	0.8	1	1.2
$R_{\max}$	1/2		
$\Phi^{(1)}$	0.404	0.393	0.323
$\Phi^{(3)}$	0.430	0.401	0.368

The search for a local maxima is carried out by a direct variational method. The flat coordinate z_1 is approximated by a truncated Fourier expansion

$$z_1 = b_0 + \sum_{n=1}^{N} [a_n \sin(n\Omega t) + b_n \cos(n\Omega t)] \qquad (24)$$

The associated flux is denoted by $\Phi^{(N)}$. For reasons of simplicity, we set $N = 3$ and $b_0 = 1$. Thus, the flux is a function of six Fourier coefficients, $\Phi = \Phi^{(3)}(a_1, a_2, a_3, b_1, b_2, b_3)$ subject to the side constraint C2. Optimal local solutions are numerically found using a simplex method [17]. Tab. 1 enumerates the achieved fluxes $\Phi^{(1)}$ with an optimal sinusoidal flat coordinate z_1 and $\Phi^{(3)}$ based on expansion (24). Near the natural frequency $\Omega = 1$, the higher harmonics of the optimal solution change sign, i.e. vanish and the fluxes are nearly equal. At lower and higher frequencies the higher harmonics help to improve the flux by roughly 10% to 20%.

The vortex and particle motion are illustrated in Fig. 3 for the optimal numerical solutions. The stable and unstable manifolds of the fixed points of the Poincaré map Φ_T are shown.

Apparently, the inclusion of the higher harmonics in

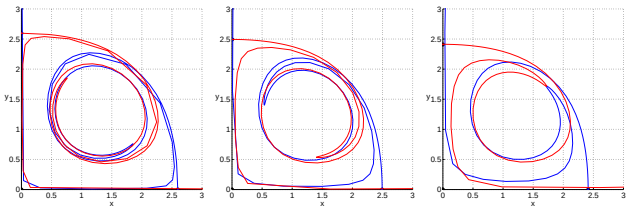

Figure 3: *Results for the optimal solution at* $\Omega = 0.8$, 1, *and* 1.2 *(left to right) and at* $R_{\max} = 0.5$. *For details see text.*

the optimization problem has little effect at $\Omega = 1$ but extends the orbits closer to the constraining circle at $\Omega \neq 0$. The actuation ϵ is largest close to the origin at $\Omega = 0.8$ while actuation is largest away from the origin at $\Omega = 1.2$. The instantaneous flux associated with vortex positions close to the origin decreases with increasing Ω, indicating that the larger averaged flux Φ may partly be due to the free-stream actuation. Another contribution may arise from the fact that the curve C moves away from the origin as Ω decreases. Thus, the instantaneous flux through C increases with decreasing frequency when the vortex is closest to the origin. In the residence time distributions, three regions can be clearly distinguished: the trapped region around the vortex, a mixing region inside the recirculation region where most of the particles leave during the first period, and a free outer region. The trapped region corresponds in the Poincaré map to the region which is embraced by the lobes of W_s and W_u.

5 Mixing dynamics and statistics

In the preceding section, controlled vortex motion which locally maximizes flux were presented. In this section, focus is placed on the dynamics of mixing employing dynamical systems theory.

The iso-contourlines of the residence time distribution and the shape of the invariant manifolds of the Poincaré map display many similarities for the optimal controlled motion (Fig. 3). These similarities are based on rigorous results of dynamical systems theory [18]. The lobe of the stable manifold W_s contains the fluid which leaves the recirculation region R during one period of the Poincaré map (Fig. 2). This fluid is bounded by the first intersection point, the W_s-lobe and the initial W_u section. The lobe of the unstable manifold W_u contains the fluid which enters R during the same interval. This fluid is bounded by the first intersection point, the W_u-lobe and the initial W_s section. Hence, the intersection of both areas identifies the fluid which enters and leaves during the considered time interval, i.e. the area between invariant manifolds connecting intersection points 2 and 3. Thus, the total fluid exchange $T_{\rm per}\,|R|\Phi$ during one period is represented by the areas bounded by C and both lobes, W_s, W_u, counting the overlap area twice. The region around the vortex which is embraced by both lobes neither leaves nor enters the recirculation zones during the considered period. The embraced region can roughly be identified as the trapped region neglecting convection effects due to the thin higher-order lobes near the axes (not resolved by present computations).

The conclusions from the studies of Poincaré maps are corroborated by a statistical analysis of fluid motion. For this analysis $\Phi_t(A)$ represents the region covered by the fluid particles at time t which were initially in A at $t = 0$. The residence coefficient $\alpha(t)$ is defined by the fraction of the fluid initially in the recirculation region R which has remained or returned to this region at time t. Let the absolute sign $|\quad|$ denote the area of a region, then the residence coefficient is expressed by

$$\alpha(t) = \frac{|\Phi_t(\mathcal{R}) \cap \mathcal{R}|}{|\mathcal{R}|}. \qquad (25)$$

Fig. 4 (top) displays the residence coefficient for the vortex motion corresponding to $R = 0.2$. The coefficient corresponding to $\Omega = 0.8$ almost converges to the asymptotic behaviour in one period, i.e. most of fluid either leaves R for ever or is trapped for infinite time. This behavior was inferred from the large overlap region between the W_s and W_u lobes of the Poincaré map. One the other hand, at $\Omega = 1.2$, the transient phase is much longer, i.e. a significant fraction of the fluid particles stays in R for one or several periods before it eventually leaves. This dynamics was concluded from the small overlap region of the invariant manifold lobes of the Poincaré map. Fig. 4 (bottom) illustrates the distribution function of the residence time. The underlying ensemble consists of the fluid particles which was initially in R at $t = 0$ and which have left R two periods later.

6 Conclusion

We have examined a problem that we deem typical in the subject of controlled fluid mixing. In particular, the control affects the velocity field but the objectives are specified in terms of particle motion. Enhanced mixing has been achieved in a recirculation zone using a vortex model for the natural and forced dynamics and employing control theory to prescribe the vortex motion. Controllability has been exploited to formulate an optimal mixing problem under suitable side constraints. Thus, the shape of the orbits have been modified by control laws to enhance mixing. The effect of actuation on hydrodynamic mixing has been derived from the invariant manifolds of Poincaré maps at periodic vortex

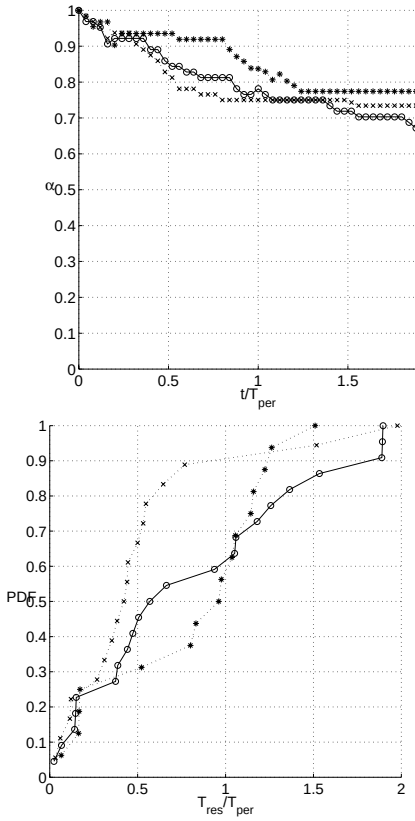

Figure 4: *Residence coefficient $\alpha(t)$ (top) and probability distribution of the residence time (bottom) for the controlled motion with $R = 0.2$ and $\Omega = 0.8$ ('x'), $\Omega = 1$ ('$\circ$') and $\Omega = 1.2$ ('$*$').*

motion. For instance, the regions of in- and outgoing fluid, the fluid exchange across the recirculation region, the region of the trapped fluid, and the residence time distribution have thus been elucidated.

The present study allows to enhance time-averaged flux by the order of 10% incorporating higher harmonics in the flat coordinate. The size of the mixing region and the flux is approximately proportional to the amplitude of oscillation at constant frequency. The area embraced by the lobes of both invariant manifolds increases strongly with increasing amplitude. Thus, the average residence time decreases with increasing flux. At large amplitudes, most fluid particles stay in the recirculation region for times of the order of 1 period. However, the overlap area between both manifolds can be decreased at nearly constant mixing region with small changes of the frequency. Thus, the flux and the average residence time can to some extend be independently controlled by suitably chosing the desired vortex motion and the corresponding control laws. This possibility represents a clear advantage over the concept of periodic open-loop forcing, in which the frequency difference between the natural and the forcing frequency may lead to quasi-periodic beat phenomena. Periodic vortex motion at non-natural frequencies cannot be excited. The class of controlled vortex motions is significantly larger than the class associated with periodic forcing.

The fluid dynamics of a recirculation region is highly idealized by the present vortex model. For instance, the shear-layer dynamics at the upper stagnation point has been shown to be of large importance at backward-facing steps [11] and in dump combustors [13], but this effect is neglected in the present study. Similarly, the non-negligible effect of turbulent fluctuations is not considered. Experiments of periodically forced flow behind a backward facing step give rise to velocity fields periodic in time, similar to the ones presented here. This similarity includes, for instance, the behaviour of the instantaneous separating streamline and the motion of the lower separation point [3]. Some observed features of the Lagrangian mixing dynamics can hence be expected to be generic for a large class of recirculation regions. These features include the fluid intake near the separation point at the lower wall, the fluid discharge near the separation point at the vertical wall and the long (ideally: infinite) residence time of the fluid trapped around the vortex, neglecting viscous and turbulent diffusion effects. Hence, several conclusions from the present control study can be expected to qualitatively hold in real flows.

Numerous generalizations of the present framework may be envisioned and may help to guide industrial applications. Control of coherent shear-layer structures under longitudinal and transverse actuation may be investigated in a similar manner with point vortices or vortex blobs. Present investigations at UTRC [14] indicate that the excitation of certain vortex configurations are beneficial for transversal mixing and pressure recovery in high-Reynolds number diffuser flows. Actuation employing control theory for higher-dimensional vortex methods require a re-formulation in the problem [6][4][5]. For instance, control laws need not necessarily depend on a single vortex position, but may be based on properties of an ensemble of vortices, of an ensemble of fluid particles or of the instantaneous velocity field sensed at one or more locations. For higher-dimensional vortex methods the 'receding horizon technique' in which a quantity is optimized over a finite period of time, might be employed. In addition, optimization strategies for actuator positions may be carried out in the present framework. Current research in this direction is in progress.

Acknowledgments

We appreciate valuable stimulating discussions with Luca Cortelezzi, Ahmed Ghoniem, George Haller, John Hauser, Gilead Tadmor, Phil Holmes, Anatoly Neishstadt, Jeff Cohen, Satish Narayanan, and Bill Proscia. This work was supported by the Air Force Office for the Scientific Research Grant F49620-98-C-0006 under program manager Mark Jacobs.

References

[1] H. Aref. Stirring by chaotic advection. *Journal of Fluid Mechanics*, 143:1–21, 1984.

[2] V.I. Arnold, Kozlov. V.V. and A.I. Neishtadt. *Mathematical aspects of classical and celestial mechanics.* Springer Verlag, Berlin, N.Y., 1988. Theorem and remark after Theorem 17,chapter 5, Sec. 3.3.

[3] J.M. Cohen. *Transient Flow over a Backward-Facing Step.* PhD thesis, The University of Conneticut, 1995.

[4] L. Cortelezzi. Nonlinear feedback control of the wake past a plate with a suction point on the downstream wall. *J. Fluid Mech.*, 327:303–324, 1996.

[5] L. Cortelezzi, Y.-C. Chen, and H.-L. Chang. Nonlinear feedback control of the wake past a plate: from a low-order model to a high-order model. *Phys. Fluids*, 9:2009–2022, 1997.

[6] L. Cortelezzi, A. Leonard, and J.C. Doyle. An example of active circulation control of the unsteady separated flow past a semi-infinite plate. *J. Fluid Mech.*, 260:127–154, 1994.

[7] D. D'Alessandro, M. Dahleh, and I. Mezić. Control of mixing in fluid flow: A maximum entropy approach. *IEEE Transactions on Automatic Control*, 44:1852–1863, 1999.

[8] M. Fliess, J. Lévine, P. Martin, and P. Rouchon. On differentially flat nonlinear systems. In *Proceedings of the IFAC Nonlinear Control Systems Design Symposium (NOLCOS)*, pages 408–412, Bordeaux, France, 1992.

[9] G.O. Fountain, D.V. Khakhar, I. Mezic, and J.M. Ottino. Chaotic mixing in a bounded three dimensional flow. *Journal of Fluid Mechanics*, 147:265–301, 2000.

[10] J. Guckenheimer and P. Holmes. *Nonlinear Oscillations, Dynamical Systems, and Bifurcation of Vector Fields.* Springer, New York, 1986.

[11] K.R. McManus, U. Vandsburger, and C.T. Bowman. Combustor performance enhancement through direct shear layer excitation. *Combustion and Flame*, 82:75–92, 1990.

[12] I. Mezić and S. Wiggins. On the integrability and perturbation of three dimensional fluid flows with symmetry. *Journal of Nonlinear Science*, 4:157–194, 1994.

[13] H.N. Najm and A.F. Ghoniem. Numerical simulation of the convective instability in a dump combustor. *AIAA J.*, 29:911–919, 1991.

[14] S. Narayanan, B.R. Noack, A. Banaszuk, and A.I. Khibnik. Dynamic separation control in 2D diffuser. Technical report, United Technologies Research Center, 1999.

[15] H. Nijmeijer and A.J. van der Schaft. *Nonlinear Dynamical Control Systems.* Springer–Verlag, New York, 1990.

[16] J.M. Ottino. *The Kinematics of Mixing: Stretching, Chaos and Transport.* Cambridge University Press, Cambridge, 1989.

[17] W.H. Press, B.P. Flamery, S.A. Teukolsky, and W.T. Vetterling. *Numerical Recipes, The Art of Scientific Computing.* Cambridge University Press, New York, New Rochelle, Melbourne, Sydney, 1986.

[18] V. Rom-Kedar, A. Leonard, and S. Wiggins. An analytical study of transport, mixing and chaos in unsteady vortical flow. *J. Fluid Mech.*, 214:347–394, 1990.

[19] Y.K. Suh. Periodic motion of a point vortex in a corner subject to a potential flow. *J. Phys. Soc. Jap.*, 62(10):3441–3445, 1993.

[20] D. V. Treschev. Width of stochastic layers in near-integrable, two-dimensional symplecic maps. *Physica D*, 116:21, 1998.

[21] S. Wiggins. *Chaotic Transport in Dynamical Systems.* Springer-Verlag, New York, 1992.